View metadata, citation and similar papers at core.ac.uk

brought to you by CORE

provided by Creative Repository of Electro-Communications

国立大学法人電気通信大学 / The University of Electro-Communications

Evaluation of the inter-particle distance of gold nanoparticles dispersed on silane-treated substrates to fabricate dithiol-connected arrays

著者（英）	Tomoki Yagai, Kazuhiko Matsumoto, Makoto Moribayashi, Masataka Moriya, Hiroshi Shimada, Ayumi Hirano-Iwata, Fumihiko Hirose, Yoshinao Mizugaki
journal or publication title	Japanese Journal of Applied Physics
volume	58
number	SD
page range	SDDF09-1-SDDF09-6
year	2019-06-01
URL	http://id.nii.ac.jp/1438/00009293/

doi: 10.7567/1347-4065/ab1476

Evaluation of the Inter-Particle Distance of Gold Nanoparticles Dispersed on Silane-Treated Substrates to Fabricate Dithiol-Connected Arrays

Tomoki Yagai[1*], Kazuhiko Matsumoto[1], Makoto Moribayashi[1], Masataka Moriya[1], Hiroshi Shimada[1], Ayumi Hirano-Iwata[2], Fumihiko Hirose[3], and Yoshinao Mizugaki[1]

[1] *Graduate School of Informatics and Engineering, The University of Electro-Communications, 1-5-1 Chofugaoka, Chofu, Tokyo, 182-8585 Japan*

[2] *Advanced Institute for Materials Research and Research Insititute of Electrical Communication,Tohoku University, 2-1-1 Katahira, Aoba-ku, Sendai, 980-8577 Japan*

[3] *Graduate School of Science and Engineering, Yamagata University, 4-3-16 Jonan, Yonezawa, Yamagata, 992-8510 Japan*

[*]E-mail: yagai@w8-7f.ee.uec.ac.jp

Small tunnel junctions using gold nanoparticles (GNPs) as electrodes have been studied to fabricate single-electron devices. GNPs connected via dithiol molecules have been used as small tunnel junctions, and a two-stage dispersion method was used to fabricate dithiol-connected GNP arrays. In this process, the GNPs were fixed on silane-treated substrates by immersing the substrate in a colloidal gold solution. For fabricating dithiol-connected arrays, the inter-particle distance of the dispersed GNPs must be smaller than the GNP diameter. Consequently, the inter-particle distance controlled by the immersion time (T_{IM1}) was evaluated. For T_{IM1} values exceeding 8 h, the inter-particle distance was less than the GNP diameter. A second dispersion of GNPs after treating samples with dithiol realized particle connections. For the GNP arrays produced with T_{IM1} values greater than 8 h, the *I–V* characteristics were measured at 77 K, and the yield of devices exhibiting nonlinear *I–V* curves was 23%.

1. Introduction

Single-electron devices have received increasing attention because of their low power consumption and high charge sensitivity.[1–5] Small tunnel junctions allow these devices to operate at higher temperatures. Therefore, single-electron devices using gold nanoparticles (GNPs) as island electrodes have been widely reported.[6–10] With the incorporation of GNPs, high-temperature operation (i.e., over 77 K, the temperature of liquid nitrogen) has been observed.[11,12] To fabricate tunnel junctions using GNPs, thiol molecules have been used as a tunneling barrier; in this process, the thiol's sulfhydryl group binds to the gold surface, and the thiol molecules form self-assembly monolayers (SAMs) on gold electrodes or GNP surfaces.[13–15] Dithiol molecules are used as a tunneling barrier because they can link GNPs. In GNPs connected via dithiol, single-electron charging effects have been observed.[16–23]

Single-electron devices that use randomly placed GNPs are generally fabricated in the following manner. A colloidal gold solution containing GNPs is repeatedly dropped on a substrate on which electrodes with a submicron gap have been previously fabricated. GNP arrays are formed within the gap of electrodes, and single-electron charging effects are observed.[24–26] This method is relatively simple. However, the GNPs may move after fabrication since the particles are not chemically fixed on the substrate. Thus, the reproducibility of these experiments is low. In addition, residues from the colloidal gold solution may remain after the sample has dried. Treating the substrate with silane is an effective approach for resolving these issues. Silane treatment of a substrate has been shown to immobilize the particles.[27–29] Then, residues on the substrate are expected to be removed by rinsing.

In this work, a two-stage dispersion method was developed to fabricate dithiol-connected GNP arrays.[30–33] Process flow of the two-stage dispersion method is shown in Fig. 1. GNPs were dispersed on silane-treated substrates by immersion in a colloidal gold solution (the first dispersion). For this dispersion step, GNPs were regularly aligned two dimensionally using the effect of an electric double layer (EDL).[28] Since GNP connections cannot be obtained with only one dispersion step, the GNPs were dispersed again after the samples were treated with dithiol (the second dispersion). The connection of the initially dispersed GNPs via a second dispersion step results in the formation of dithiol-connected GNP arrays. In addition, to fabricate dithiol-connected arrays, the inter-particle distance of the initially

dispersed GNPs must be smaller than the diameter of the secondarily dispersed GNP, where the inter-particle distance is defined as the distance from the edge of one particle to the edge of another particle, as shown in Fig. 3(a). Hence, this distance was evaluated and controlled by changing the immersion time (T_{IM1}) for the first dispersion. The current–voltage (I–V) characteristics were measured for the fabricated GNP arrays, and finally, the yield of devices exhibiting nonlinear I–V curves was determined.

2. Experimental methods

The first dispersion was conducted in the following manner. [Step 1] NiCr/Au electrodes with gaps were fabricated on Si substrates covered by SiO_2 (1 μm) using electron beam lithography, shadow evaporation, and a lift-off process. In the shadow evaporation, the angle for NiCr evaporation was smaller than that for Au evaporation to prevent the NiCr layer from exceeding the Au layer at the tips around the gap. The gap length was 50–300 nm, and the electrode thickness at the tip was 20 nm on one side and 45 nm on the other side. Schematic side-view and top-view illustrations of the electrode gap are shown in Fig. 1(a). [Step 2] The samples were immersed in acetone and ethanol for surface cleaning. Subsequently, the samples were immersed in a 1% (v/v) aqueous solution of (3-aminopropyl)-triethoxysilane for 10 min and rinsed in deionized water. [Step 3] The samples were immersed in a colloidal gold solution and rinsed in deionized water. The GNPs in colloidal gold solution were stabilized by citrate. The nominal GNP diameter was 30 nm. The immersion in colloidal gold solution was performed at 5 ℃. Figure 1(b) shows a schematic illustration of the sample after the first dispersion. The particle coverage was determined from scanning electron microscopy (SEM) images of the dispersed GNPs. The ImageJ software was used to binarize the SEM images and to assess the particle coverage.

The second dispersion was conducted in the following manner. After the first dispersion, the samples were immersed for more than 18 h in 5 mM 1,10-decanedithiol ethanol solution and then rinsed with ethanol. Next, the samples were immersed in a colloidal gold solution for 6 h and rinsed in deionized water. The colloidal gold solution was the same as that used in the first dispersion. The immersion in colloidal gold solution was performed at 5 ℃. The fabricated devices were observed using SEM. The I–V characteristics of the devices were measured at 77 K, and particle connections within the gap were confirmed. Figure 1(c)

shows a schematic illustration of the fabricated device with the measurement circuit after the second dispersion.

3. Results and discussion

3.1 Evaluation of the inter-particle distance of the initially dispersed GNPs

Figure 2(a) shows SEM images of typical GNPs attached to a substrate after the first dispersion. In all images, the GNPs were regularly aligned two-dimensionally, although some aggregations of GNPs were also observed. With increasing T_{IM1}, the number of GNPs increased. Figure 2(b) shows an SEM image of a sample that was not treated with silane for T_{IM1} = 8 h. The number of GNPs on the substrate is smaller than that on the silane-treated sample. Figure 2(c) shows the particle coverage plotted as a function of T_{IM1}. Particle coverages were obtained on several areas for each sample, and each data point in Fig. 2(c) corresponds to a single sample. The error bars denote the standard deviation. The particle coverage increased monotonically for T_{IM1} values of 1–10 h and was saturated for values exceeding 10 h. The particle coverage for T_{IM1} = 18 h is lower than that for 10 and 14 h because the SEM image is distorted at high particle densities, and the particle coverage contains a larger error than those shown by the error bars.

By assuming that the GNP arrangement is a two-dimensional triangular lattice, the inter-particle distances were estimated from the particle coverage. Figure 3(a) shows a schematic model of the two-dimensional triangular lattice, where the GNP radius is labeled as r. For the inter-particle distance d was calculated using Eq. (1).

$$N = \frac{2\pi r^2}{\sqrt{3}(d+2r)^2} \qquad (1)$$

where N is the particle coverage. Figure 3(b) shows the dependence of the inter-particle distance d on T_{IM1}. As T_{IM1} increased to 10 h, the inter-particle distance increased; beyond this value, the inter-particle distance was virtually constant. The value of d for T_{IM1} = 18 h was estimated to be 23.6 nm using Eq. (1). For comparison, the inter-particle distances were actually measured for the dispersed GNPs with T_{IM1} = 18 h. Figure 4(a) presents an SEM image of the GNPs after the first dispersion. For the region denoted by a dashed line, inter-particle distances were actually measured via SEM. Figure 4(b) shows a histogram of the measured inter-particle distances, with an intermediate value of 21–24 nm. Since the estimated inter-particle distance for T_{IM1} = 18 h was within the measured range at 23.6 nm,

the assumption that the GNP arrangement is a two-dimensional triangular lattice is reasonable.

To compare the EDL length with the estimated inter-particle distance, the EDL length surrounding a GNP was calculated as follows.[28,34] The hydrogen ion concentration was calculated as 3.3×10^{-4} nm^{-3} at a pH of 3.26, which was the pH of the colloidal gold solution as measured by a pH meter. Assuming that all citrate ions were trivalent and that the solution was electrically neutral, the citrate ion concentration was calculated as 1.1×10^{-4} nm^{-3}. The ionic strength of the solution I is given by

$$I = \frac{1}{2}\sum_i n_i Z_i^2 \qquad (2)$$

where n_i and Z_i represent the concentration of the ionic species and the valence number of the ions, respectively. The calculated value of I was found to be 6.6×10^{-4} nm^{-3}. The length of the EDL λ is given by

$$\lambda = \sqrt{\frac{\varepsilon kT}{e^2 I}} \qquad (3)$$

where ε, k, T, and e are the dielectric constant of the solution, Boltzmann constant, absolute temperature, and unit charge, respectively. If we assume that the minimum inter-particle distance is twice the magnitude of λ, the calculated value of 2λ can be estimated as 25 nm. This value is consistent with the estimated inter-particle distance of 23.6 nm for T_{IM1} = 18 h. This result suggests that the saturation of the inter-particle distance is caused by the EDL.

To obtain particle connections via a second dispersion step, the inter-particle distance must be less than 30 nm, which is the diameter of the secondarily dispersed GNP. For T_{IM1} values exceeding 8 h, the estimated inter-particle distances were smaller than 30 nm; therefore, a connection among the GNPs is expected after the second dispersion step.

3.2 Particle connection via a second dispersion step

Figures 5(a) and 5(b) display images of GNPs attached to a substrate before and after the second dispersion. The T_{IM1} of this sample was 8 h, and the two images were obtained from different areas of a sample with no electrodes. Figures 5(c) and 5(d) display binarized SEM images of Figs. 5(a) and 5(b), respectively. Figures 6(a) and 6(b) present histograms of the particle area before and after the second dispersion, where the particle area was defined as the area occupied by a continuous black region in a binarized SEM image as shown in Figs.

5(c) and 5(d). Each particle area value was derived from binarized SEM images using the ImageJ software.

In Fig. 6(a), peaks occur in the ranges of 600–800 and 1200–1600 nm^2. The top-view area of a single particle is 707 nm^2, as calculated from the GNP diameter (30 nm). Hence, these peaks correspond to single particles and aggregations of two particles, respectively. The total frequencies in the range of 600–800 nm^2 in Figs. 6(a) and 6(b) were 467 and 72, respectively. The frequency in this range decreased dramatically after the second dispersion, indicating that virtually all individual GNPs were connected via dithiol after the second dispersion.

3.3 Electric properties of the fabricated GNP arrays

Figure 7(a) shows an SEM image of a fabricated device after the second dispersion process. Connected GNP arrays were observed in the gap between electrodes. For this device, T_{IM1} was 18 h. Figure 7(b) shows an *I–V* curve measured at 77 K for the device. A nonlinear *I–V* curve was observed for this device, as shown in Fig. 7(b). The differential conductance in the region of $|V| \geq \pm 2.6$ V was found to be 0.12 nS. The tunneling conductance for mixed SAMs of octanedithiol and decanedithiol is 0.5 nS or higher,[35] which is larger than the measured conductance, indicating that several GNPs were connected in series in the gap between electrodes.

To fabricate GNP arrays, an immersion time of 6 h was implemented for the second dispersion, with T_{IM1} values exceeding 8 h. The *I–V* characteristics of the devices were measured at 77 K. Among 30 fabricated devices, 7 and 2 devices exhibited nonlinear and linear *I–V* curves, respectively, and for 21 devices, the gap between electrodes were not electrically connected. Thus, the yield for devices exhibiting nonlinear *I–V* curves was 23%. This yield may be low because some of the inter-particle distances were larger than 30 nm, as shown in Fig. 2(b), and because there are variations in the GNP diameter.

4. Conclusions

To fix GNPs, substrates were treated with silane. GNPs were dispersed on the substrates by immersion in a colloidal gold solution. The particle coverage increased monotonically for T_{IM1} values of 1–10 h and was saturated for T_{IM1} values exceeding 10 h due to the effect of the EDL. To obtain particle connections via a second dispersion step, the inter-particle

distance must be less than 30 nm, which is the diameter of the secondarily dispersed GNPs. The estimated inter-particle distance for T_{IM1} values exceeding 8 h was less than 30 nm. After the samples were treated with dithiol, devices were fabricated by a second GNP dispersion step. Histograms of the particle area before and after the second dispersion were compared. The frequency of individual particles decreased dramatically after the second dispersion, indicating that virtually all single GNPs were connected via dithiol after the second dispersion step. For T_{IM1} values exceeding 8 h, nonlinear *I–V* curves were observed in 23% of the devices.

Acknowledgments

This work was partly supported by JSPS KAKENHI Grant Number 17K04979, and by JST-CREST Grant Number JPMJCR14F. Nation-wide Cooperative Research Projects, Research Institute of Electrical Communication, Tohoku University are also acknowledged.

References

1) T. A. Fulton and G. J. Dolan, Phys. Rev. Lett. **59**, 109 (1987).
2) U. Meirav, M.A. Kastner, S.J. Wind, Phys. Rev. Lett. **65**, 771 (1990).
3) K. K. Likharev, Proc. IEEE **87**, 606 (1999).
4) D. Berman, N. B. Zhitenev, R. C. Ashoori, H. I. Smith, and M. R. Melloch, J. Vac. Sci. Technol. B **15**, 2844 (1997).
5) L.J. Geerligs, V. F. Anderegg, P. A. M. Holweg and J. E. Mooij, Phys. Rev. Lett. **64**, 2691 (1990).
6) U. Simon, Adv. Mater. **10**. 1487 (1998).
7) A. Zabet-Khosousi and A. A. Dhirani, Chem. Rev. **108**, 4072 (2008).
8) K. I. Bolotin, F. Kuemmeth, A. N. Pasupathy, and D. C. Ralph, Appl. Phys. Lett. **84**, 3154 (2004).
9) F. Kuemmeth, K. I. Bolotin, S.-F. Shi, and D. C. Ralph, Nano Lett. **8**, 4506 (2008).
10) O. Bitton, D. B. Gutman, R. Berkovits, and A. Frydman, Nature Communications **8**, 402 (2017).
11) C. Thelander, M. H. Magnusson, K. Deppert, L. Samuelson, P. R. Poulsen, J. Nygard, and J. Borggreen, Appl. Phys. Lett. **79**, 2106 (2001).
12) H. Zheng, M. Asbahi, S. Mukherjee, C. J. Mathai, K. Gangopadhyay, J. K. W. Yang, and S. Gangopadhyay, Nanotechnology **26**, 355204 (2015).
13) R. Negishi, T. Hasegawa, K. Terabe, M. Aono, T. Ebihara, H. Tanaka, and T. Ogawa, Appl. Phys. Lett. **88**, 223111 (2006).
14) R. Negishi, T. Hasegawa, K. Terabe, M. Aono, H. Tanaka, T. Ogawa and H. Ozawa, Appl. Phys. Lett. **90**, 223112 (2007).
15) S. K. Bose, C. P. Lawrence, Z. Liu, K. S. Makarenko, R. M. J. van Damme, H. J. Broersma, and W. G. van der Wiel, Nature Nanotechnology **10**, 1048 (2015).
16) D. L. Klein, P. L. McEuen, J. E. B. Katari, R. Roth, and A. P. Alivisatos, Appl. Phys. Lett. **68**, 2574 (1996).
17) Y. Noguchi, T. Terui, T. Katayama, M. M. Matsushita, and T. Sugawara, J. Appl. Phys. **108,** 094313 (2010).
18) Y. Azuma, Y. Yasutake, K. Kono, M. Kanehara, T. Teranishi and Y. Majima, Jpn. J. Appl. Phys. **49**, 090206 (2010).

19) K. Maeda, N. Okabayashi, S. Kano, S. Takeshita, D. Tanaka, M. Sakamoto, T. Teranishi and Y. Majima, ACS Nano **6**, 2798 (2010).
20) Y. Azuma, S. Suzuki, K. Maeda, N. Okabayashi, D. Tanaka, M. Sakamoto, T. Teranishi, M. R. Buitelaar, C. G. Smith, and Y. Majima, Jpn. Appl. Phys. Lett. **99**, 073109 (2011).
21) S. Kano, Y. Azuma, K. Maeda, D. Tanaka, M. Sakamoto, T. Teranishi, L. W. Smith, C. G. Smith, and Y. Majima, ACS Nano **6**, 9972 (2012).
22) Y. Azuma, M. Sakamoto, T. Teranishi, and Y. Majima, Appl. Phys. Lett. **109**, 223106 (2016).
23) Y. Majima, G. Hackenberger, Y. Azuma, S. Kano, K. Matsuzaki, T. Susaki, M. Sakamoto, and T. Teranishi, Adv. Mater. **18**, 375 (2017).
24) M. Moriya, T. T. T. Huong, K. Matsumoto, H. Shimada, Y. Kimura, A. Hirano-Iwata, and Y. Mizugaki, Appl. Phys. A **122**, 756 (2016).
25) T. T. T. Huong, K. Matsumoto, M. Moriya, H. Shimada, Y. Kimura, A. Hirano-Iwata, and Y. Mizugaki, Appl. Phys. A **123**, 557 (2017).
26) T. T. T. Huong, K. Matsumoto, M. Moriya, H. Shimada, Y. Kimura, A. Hirano-Iwata, and Y. Mizugaki, Appl. Phys. A **123**, 268 (2017).
27) K. C. Grabar, P. C. Smith, M. D. Musick, J. A. Davis, D. G. Walter, M. A. Jackson, A. P. Guthrie, and M. J. Natan, Am. Chem. Soc. **118**, 1148 (1996).
28) L. Jiang, C. Zou, Z. Zhang, Y. Sun, Y. Jiang, W. Leow, B. Liedberg, S. Li, and X. Chen, Small **10**, 609 (2014).
29) J. Chen, J. Huang, A. Toma, L. Zhong, Z. Cui, W. Shao, Z. Li, W. Liang, F. D. Angelis, L. Jiang, and L. F. Chi, Adv. mater. Interfaces **2017**, 1700505 (2017).
30) T. Sato, H. Ahmed, D. Brown, and B. F. G. Johnson, J. Appl. Phys. **82**, 696 (1997).
31) P.-E. Trudeau, A. Escorcia, and A.-A. Dhirani, J. Chem. Phys. **119**, 5267 (2003).
32) P. U. Vivitasari, Y. Azuma, M. Sakamoto, T. Teranishi, and Y. Majima, Mater. Res. Express **4**, 024004 (2017).
33) Y. Mizugaki, K. Matsumoto, M. Moriya, H. Shimada, A. Hirano-Iwata, and F. Hirose, Jpn. J. Appl. Phys. **57**, 098006 (2018).
34) U. Schnabel, C.-H. Fischer and E. Kenndler, J. Microclumn Sep. **9**, 529 (1997).
35) X. Li, Y. Yasutake, K. Kono, M. Kanehara, T. Teranishi, and Y. Majima, Jpn. J. Appl. Phys. **48**, 04C180 (2009).

Figure Captions

Fig. 1. (Color online) Side-view and top-view schematic illustrations of the gap between electrodes. (a) Fabricated electrodes. (b) Fixed particles after the first dispersion. (c) Fabricated dithiol-connected arrays with a measurement circuit after the second dispersion.

Fig. 2. (Color online) (a) SEM images of samples with various T_{IM1} values after the first dispersion. (b) SEM image of a sample that was not treated with silane for T_{IM1} = 8 h. (c) T_{IM1} dependence of the particle coverage.

Fig. 3. (Color online) (a) Assumed GNP arrangement. (b) T_{IM1} dependence of the estimated inter-particle distance.

Fig. 4. (Color online) (a) SEM image of dispersed GNPs for T_{IM1} = 18 h. (b) Histogram of inter-particle distances in the region denoted by a dashed line in Fig. 2(a).

Fig. 5. (Color online) (a) SEM image of GNPs after the first dispersion for T_{IM1} = 8 h. (b) SEM image acquired after the second dispersion. (c) Binarized image of (a). (d) Binarized image of (b).

Fig. 6. (Color online) Particle area histograms for dispersed GNPs with T_{IM1} = 8 h. (a) Before and (b) after the second dispersion.

Fig. 7. (Color online) (a) SEM image of a device in which the gap between the electrodes was connected. (b) *I–V* characteristics of the device at 77 K.

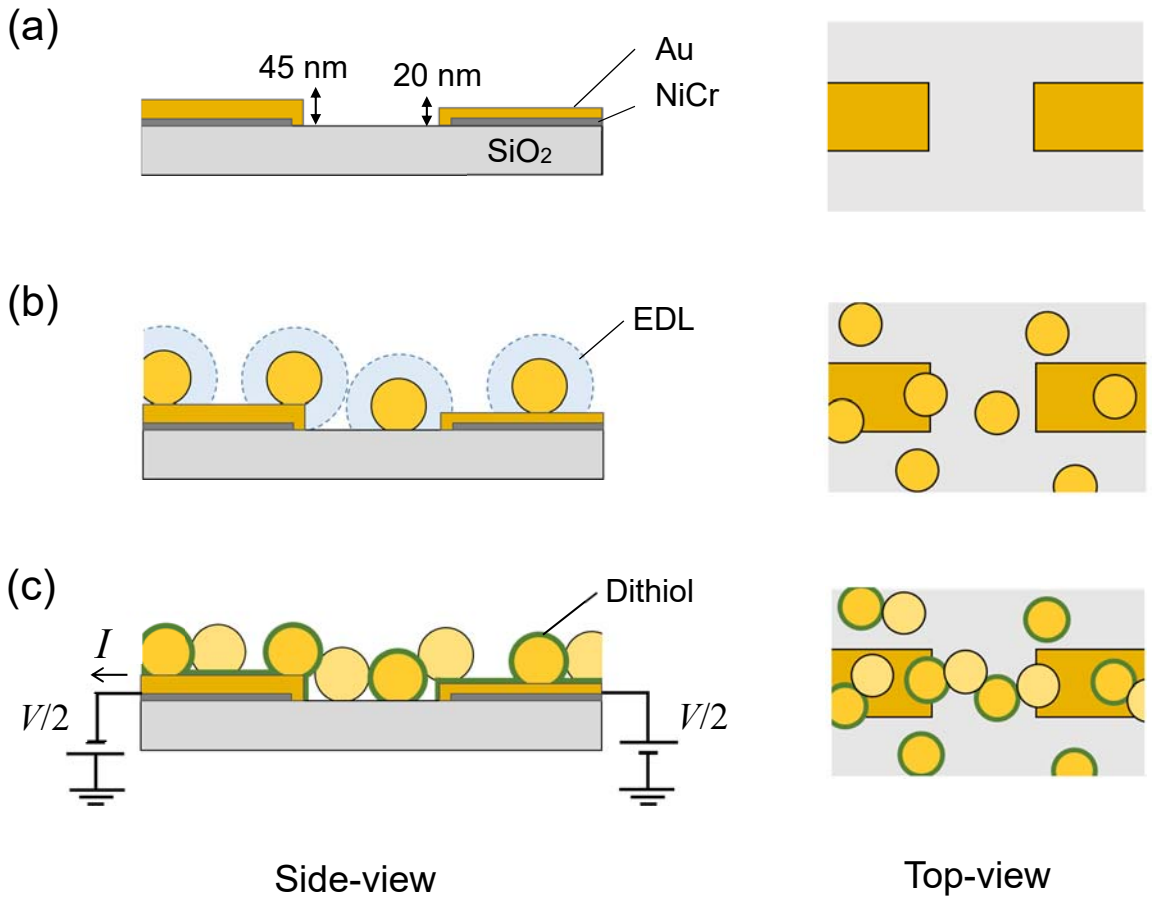

Fig. 1. (Color online)

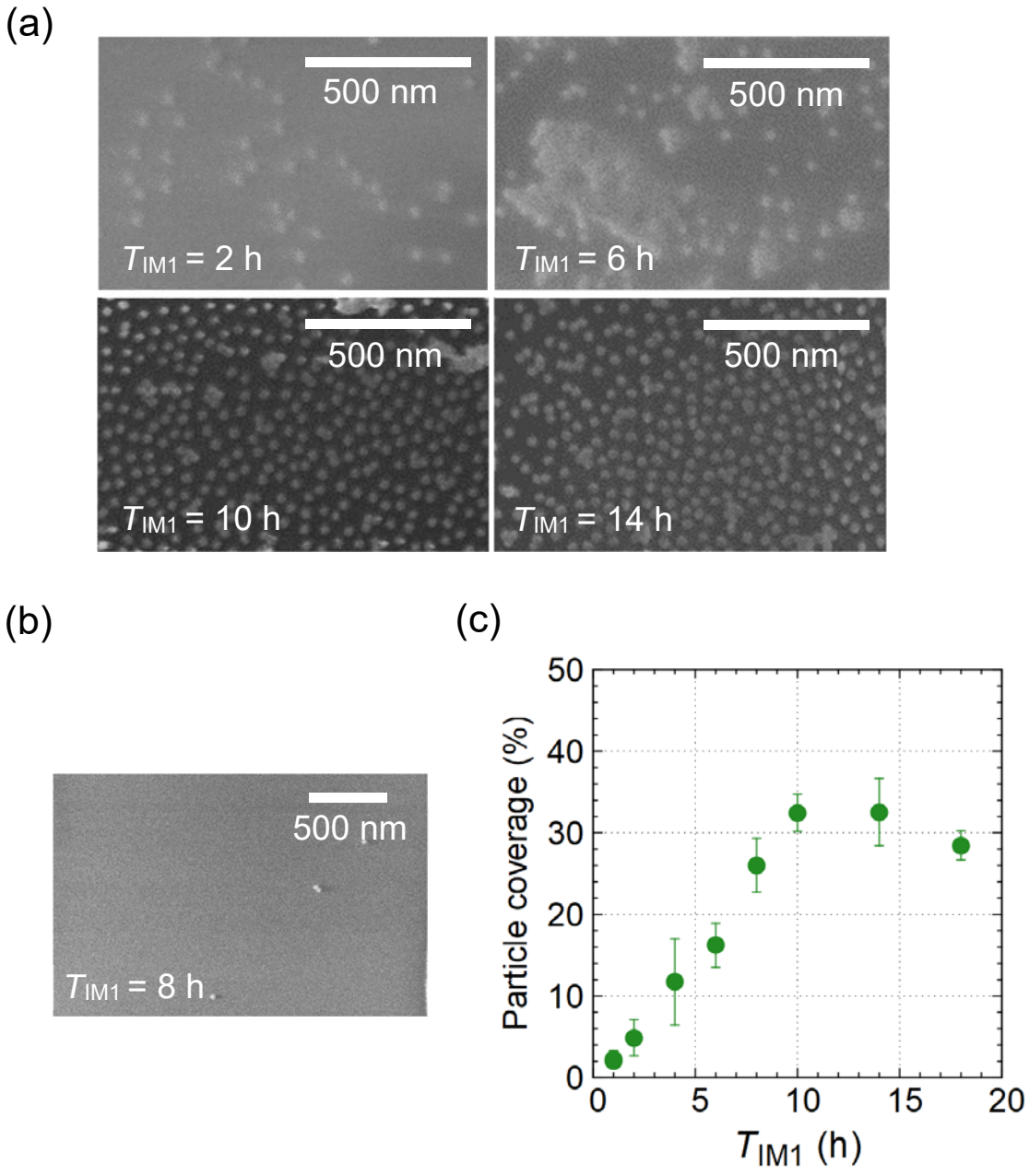

Fig. 2. (Color online)

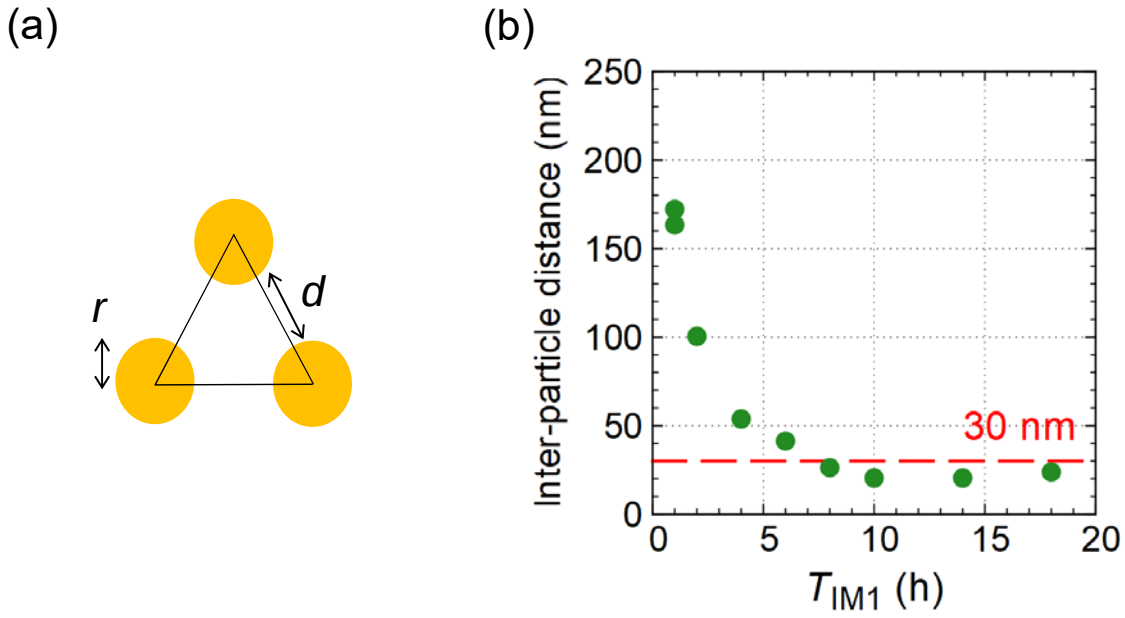

Fig. 3. (Color online)

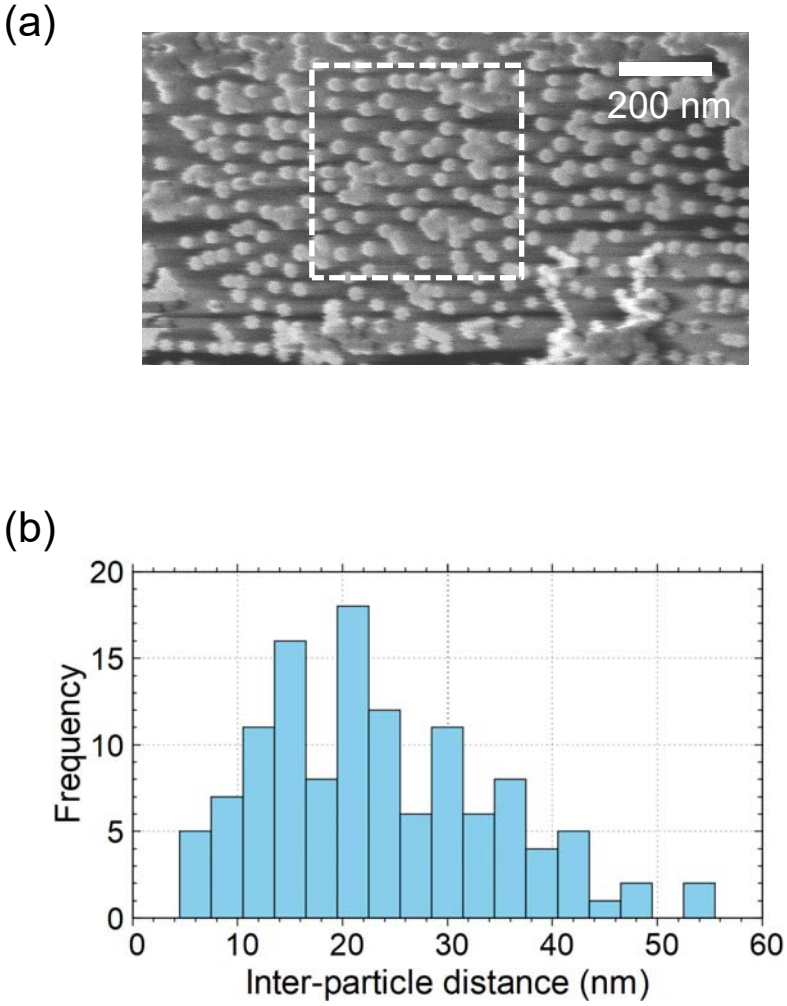

Fig. 4. (Color online)

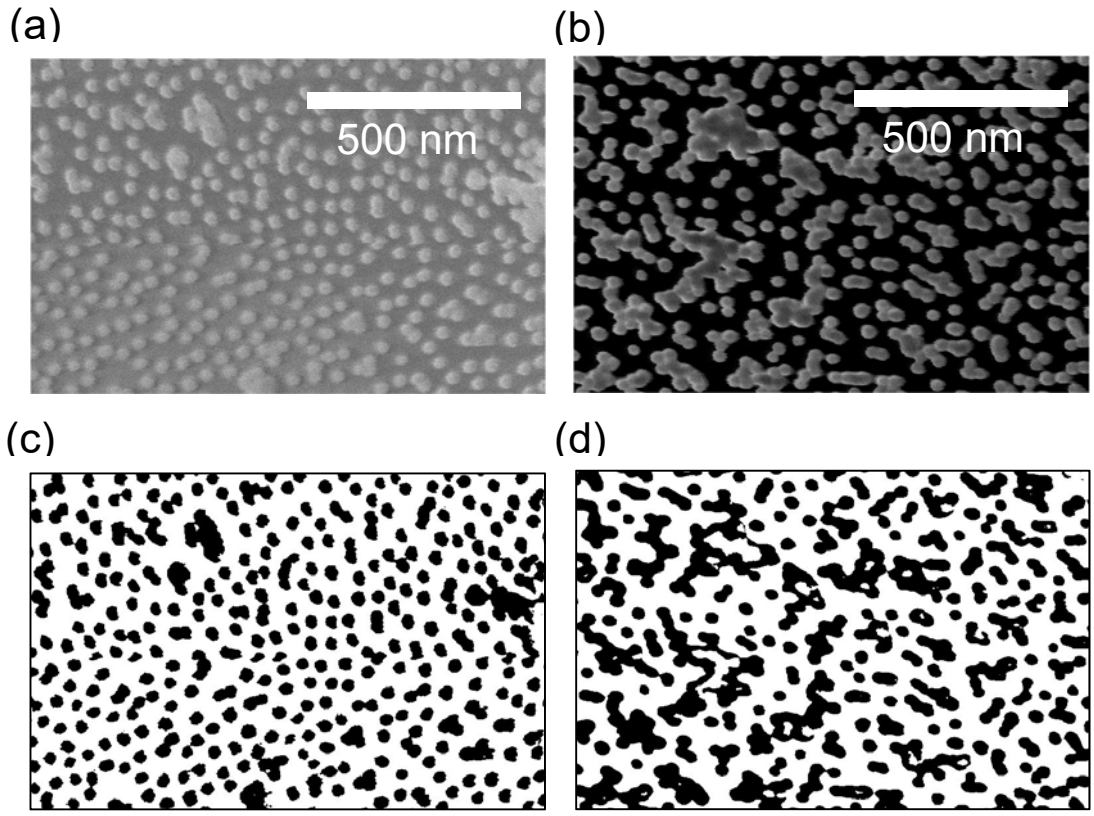

Fig. 5. (Color online)

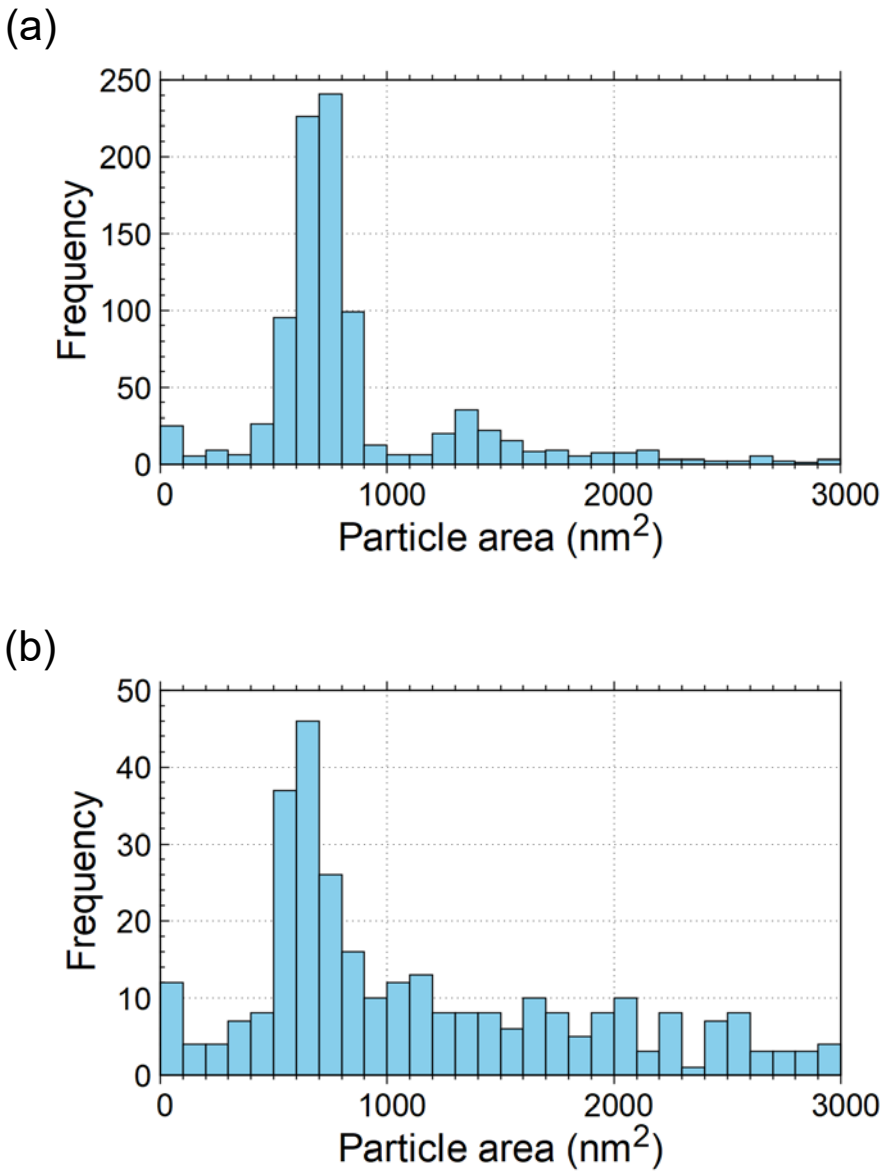

Fig. 6. (Color online)

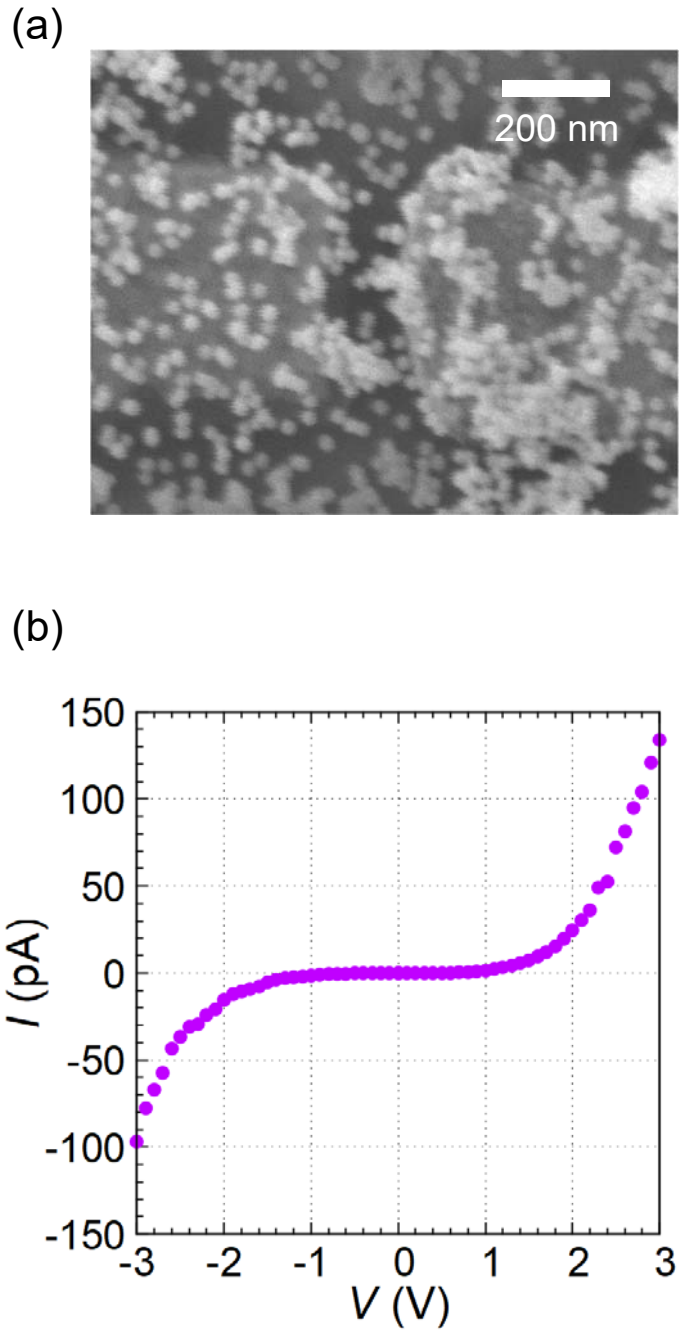

Fig. 7. (Color online)